frontiers | Frontiers in Physics

TYPE Original Research
PUBLISHED 09 December 2022
DOI 10.3389/fphy.2022.1038416

OPEN ACCESS

EDITED BY
Jinqing Yu,
Hunan University, China

REVIEWED BY
Anuraj Panwar,
Jaypee Institute of Information Technology, India
Jin-Long Jiao,
Zhejiang University, China

*CORRESPONDENCE
Yan-Yun Ma,
yanyunma@126.com

SPECIALTY SECTION
This article was submitted to Fusion Plasma Physics, a section of the journal Frontiers in Physics

RECEIVED 07 September 2022
ACCEPTED 22 November 2022
PUBLISHED 09 December 2022

CITATION
Peng M, Ma Y-Y, Li B-Y, Tian L-C, Jiang J, Zi M and Yang X-H (2022), Enhancement of positron yields using multi-layer targets irradiated by laser-induced energetic electrons.
Front. Phys. 10:1038416.
doi: 10.3389/fphy.2022.1038416

Enhancement of positron yields using multi-layer targets irradiated by laser-induced energetic electrons

Meng Peng[1], Yan-Yun Ma[2,3]*, Bo-Yuan Li[4], Li-Chao Tian[1], Jing Jiang[1], Ming Zi[1] and Xiao-Hu Yang[1]

[1]College of Science, National University of Defense Technology, Changsha, China, [2]College of Advanced Interdisciplinary Studies, National University of Defense Technology, Changsha, China, [3]Collaborative Innovation Centre of IFSA, Shanghai Jiao Tong University, Shanghai, China, [4]Key Laboratory for Laser Plasmas (MoE), School of Physics and Astronomy, Shanghai Jiao Tong University, Shanghai, China

Positrons with high energy and short pulse duration generated by the ultra-short and ultra-intense laser interaction with a two-target system (under-density plasma target and high-Z metal target) have wide applications. In this paper, we proposed an optimal scheme for enhancing positrons with multi-layer high-Z converters. Positrons with larger divergence escape from the target zone, reducing positron annihilation in the target, while secondary particles with smaller divergence react with the subsequent target to produce more positrons. The total positron yield and positron beam divergence increased obviously with the target number when using the thin converter, while the scenario was reversed for the recorded positrons. The total positrons produced by bilayer 5-mm targets and eight-layer 1-mm targets increased by 14% and 62%, respectively, compared to the outgoing positrons produced by an 8-mm monolayer target. Positron yields can be further enhanced by adjusting the thickness of the subsequent target and distance, according to the intensity and angular distribution of positrons emitted from the previous target.

KEYWORDS

ultra-intense laser, wakefield electrons, positrons, multi-layer targets, Geant4 simulation

Introduction

Positrons with relativistic energy have attracted considerable attention due to their numerous potential applications [1], such as in nuclear and particle physics, plasma physics [2], and material science [3, 4]. The ultra-short and ultra-intense laser provides an innovative new approach for generating positrons. Since the theory proposed by Shearer et al. [5] in 1973 and the invention of the chirped pulse amplification (CPA) technique [6] by Strickland and Mourou in the mid-1980s, the electron–positron pairs produced by the ultra-intense laser have been extensively investigated in great detail through theory [5, 7–13] and experiment [14–20]. Cowan et al. [21] experimentally demonstrated the ability

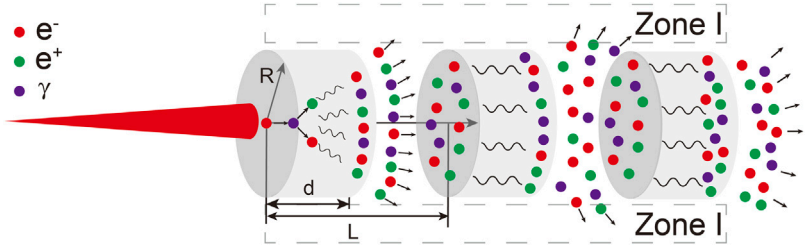

FIGURE 1
Scheme of multi-layer targets for positron enhancement.

of an ultra-intense laser pulse to produce positrons for the first time on the Nova Peta-Watt laser. As we know, the Bethe–Heitler (BH) process and the trident process are the two main methods to produce positrons through hot electrons. Previous studies have demonstrated that positron generation *via* the trident process predominates over the BH process for a thin target (<30 μm for solid gold) [7], while the scenario is reversed for a thick high-Z target [8, 9]. There is a cross point around which the dominant process switches from the trident process to the BH process that depends mainly on the plasma density and converter thickness.

In the early experiments [20, 22, 23], the positron beam based on the laser and thick high-Z target direct interaction has a higher yield and a larger divergence. However, the positron yield relies on the laser intensity and an optimum laser intensity is around 10^{21} W/cm^2 in the fixed laser energy [9]. Another alternative solution is to separate the electron generation and electromagnetic shower into two distinct stages [14, 24]. Generally speaking, the energetic electron beam is first generated by the interaction of a relatively low-intensity laser with a gaseous target; then, these electrons propagate through a high-Z solid target to produce electron–positron pairs by the BH process. The positron beam generated by such a two-target system shows some unique properties such as short pulse duration (~ps), high energy (~MeV), and high density (>10^{12} cm^{-3}). At the same time, the femtosecond laser system used in the positron experiment is more compact and easier to work in high frequency and at low cost. However, increasing the target thickness contributes to electron–positron pair annihilation that leads to a sharp decrease in the positron yield.

Here, we propose a scheme of multi-layer targets to enhance the total positrons (see Figure 1) by adding multiple targets to keep secondary particles (positrons, electrons, and γ-rays) of small divergence reacting with the subsequent target for more positron production, while the low-energy positrons of large divergence escape from the target zone (zone I), reducing the positron annihilation in the target.

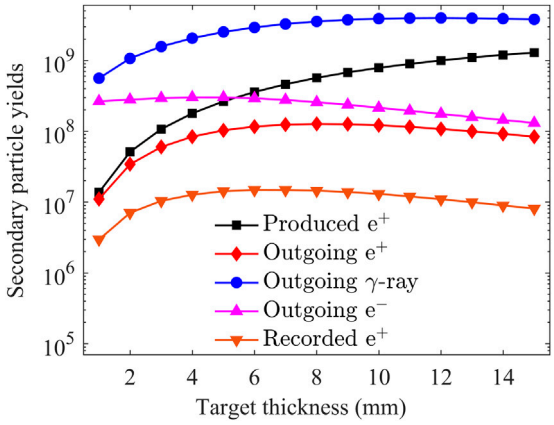

FIGURE 2
Secondary particle yields by the interaction of laser-induced energetic electron beam with tungsten target of different thicknesses.

Simulation study on positron generation

Monolayer target simulation

The distribution function of the electron–positron pair depends only on the primary electron energy E, electron number N, and the target thickness d. In this section, the transportation of electrons and electron-induced secondary particles interacting with the high-Z (tungsten) target has been studied with Geant4 (Version 4.10.7) [25, 26]. The initial electron spectrum was extracted from the previous experiment in the same experimental conditions as this article [27]. Here, we assumed that the cascade was initiated by a pencil-like electron beam of 50 mrad perpendicularly propagating to the target after a 50-cm flight path. At high energies, the cascade was assumed to propagate essentially along the initial direction of electron propagation.

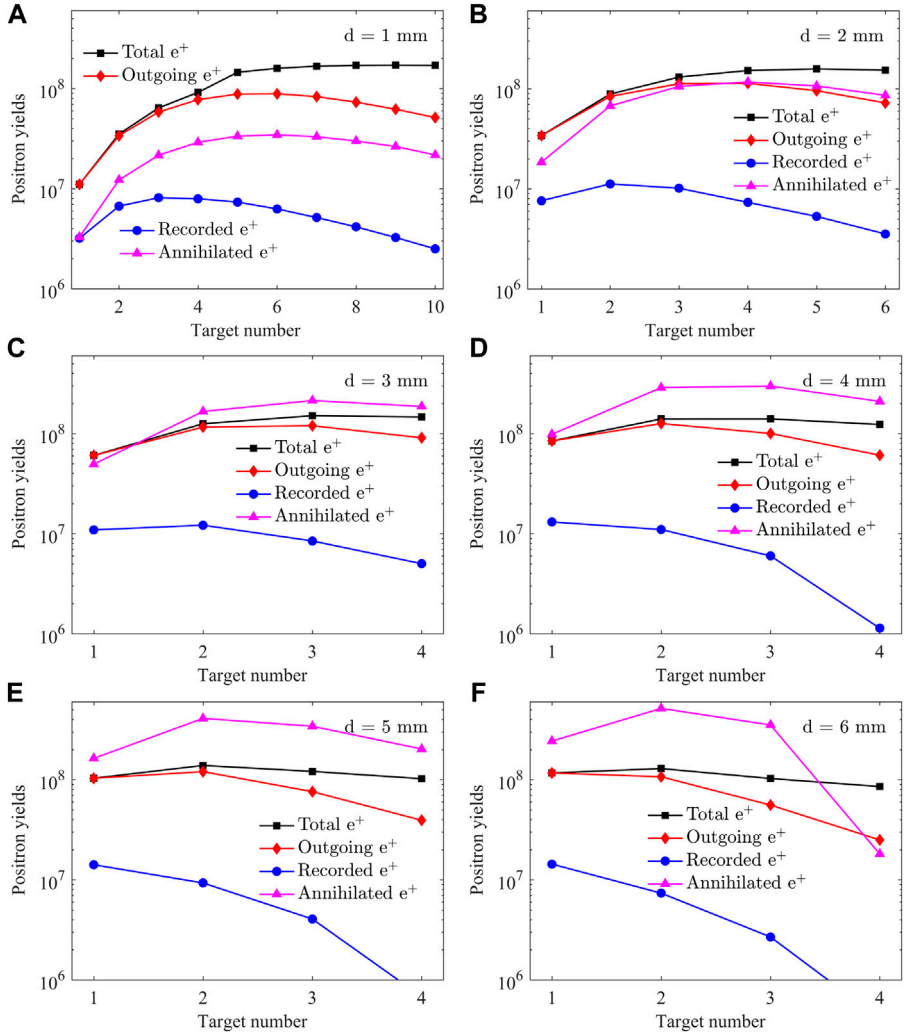

FIGURE 3
Calculated yields of the total positrons, outgoing positrons, recorded positrons, and annihilated positrons with different target numbers at a monolayer thickness of **(A)** 1 mm, **(B)** 2 mm, **(C)** 3 mm, **(D)** 4 mm, **(E)** 5 mm, and **(F)** 6 mm.

Figure 2 shows the calculated results of electron-induced secondary particles generated once an electron beam propagated through a tungsten target with a thickness ranging from 1 mm to 15 mm, which roughly covers the radiation length of tungsten ranging from 0.3 to 4. Here, we defined the produced positrons as the primary positrons without the annihilation process, the outgoing particles as these particles emitted from the front surface of the target, and the recorded positrons as these positrons over < 3° divergence and <5 mm diameter spot emitted from the front surface center of the target because these positrons can reach the magnetic field after propagation through the collimator in the actual experiment. As we can see, the maximum yields for the recorded positrons and outgoing positrons were obtained for the thicknesses of 8 mm and 6 mm, respectively, while increasing target thickness above this value induced a net decrease in positron yields. This can be intuitively understood by noting that, for such a thick target, there is a higher probability that any generated positrons within the target may undergo more energy loss during propagation through the rest of the high-Z target [17]. Electrons and positrons are also constantly moderated to the low-energy region through ionization and bremsstrahlung processes and eventually annihilate as transportation in the target, while increasing the high-Z target thickness above the threshold induces a net decrease when the annihilation process overcomes the BH process. Therefore, the outgoing electrons gradually decreased and tended to the positrons with the increasing target thickness because the outgoing electrons and positrons were mainly produced by γ-rays.

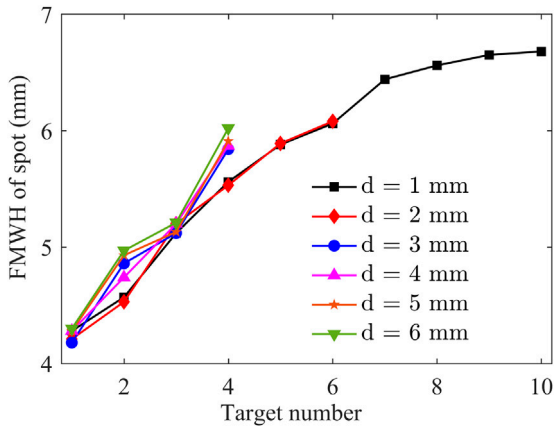

FIGURE 4
Layer-dependent FWHM of the outgoing positrons with different target numbers at a monolayer target thickness ranging from 1 mm to 6 mm.

Multi-layer target simulation

There are many factors affecting the positron yields, such as the target size *R*, target distance *L*, target thickness *d*, and target number *N*. Based on our specific experimental conditions, the ratio of $R/(L-d) = 1$ is set to study the effects of positron enhancement based on multi-layer targets at a monolayer thickness ranging from 1 mm to 6 mm on the positron yields normalized to the indent electron beam (see Figures 3A–F). Here, we defined the total positrons as the sum of scattering positrons that escaped from the target zone and outgoing positrons and defined the outgoing positrons as these positrons emitted from the front surface of the last target. The recorded positrons decreased gradually with an increase in the target number when adding more than three layers, and this phenomenon was more obvious with a thick target. Although the recorded positrons produced by multi-layer targets were significantly lower than those produced by an 8-mm monolayer target, the total positrons had a considerable enhancement by optimizing the multi-layer targets structure. The total positron yields increased with the high-Z target number until the scattering positrons were larger than the outgoing positron loss in the subsequent target. Based on the simulation results, we can obtain more positrons with the multi-layer targets. However, the positron enhancement under the thin targets (<=4 mm) with an increase in the target number became more and more obvious, while the optimal scheme for the thick target (5 mm and 6 mm) was bilayer. The full width at half maximum (FWHM) of the outgoing positron beam increased significantly to some extent with an increase in the target thickness and target number (see Figure 4). The FWHM of the positron beam was larger than the hole diameter of the collimator when adding more than two layers, preventing more positrons from entering the magnetic field. It is detrimental to positron collection emitted from the escape zone in nearly forward 2π space with an increase in the target, and the optimal solution for multi-layer targets should not exceed three layers under our specific experimental parameters.

Experiment for positron generation

Monolayer target scheme

The experimental campaign of positron production by a monolayer target was, thus, carried out at a 200 TW fs laser facility. A detailed description of the experimental setup is shown in Figure 5, where an ultra-intense laser with a peak intensity of 2.8×10^{19} W/cm^{-2}, delivered in 29 fs over a 30-μm diameter focus, was focused onto the edge of a supersonic He gas jet mixed with 0.5% N_2 with a backing pressure of 0.4 MPa. The collimator of ~1 cm diameter through 10-cm plastic (Teflon) was installed along the laser beam axis at a distance of 58 cm from the gas jet. A high-Z converter was installed close to the collimator for positron production. A magnetic spectrometer (B = 1 T, length 16 cm) close to the

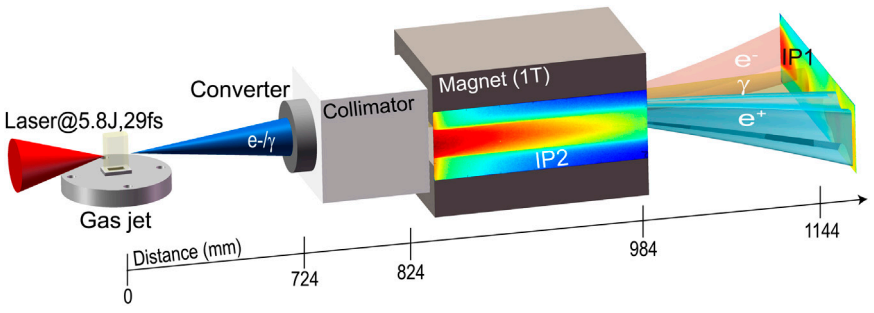

FIGURE 5
Sketch of the experimental setup for positron production. Laser-induced particles are separated by the magnetic spectrometer and then recorded onto IP1 and IP2.

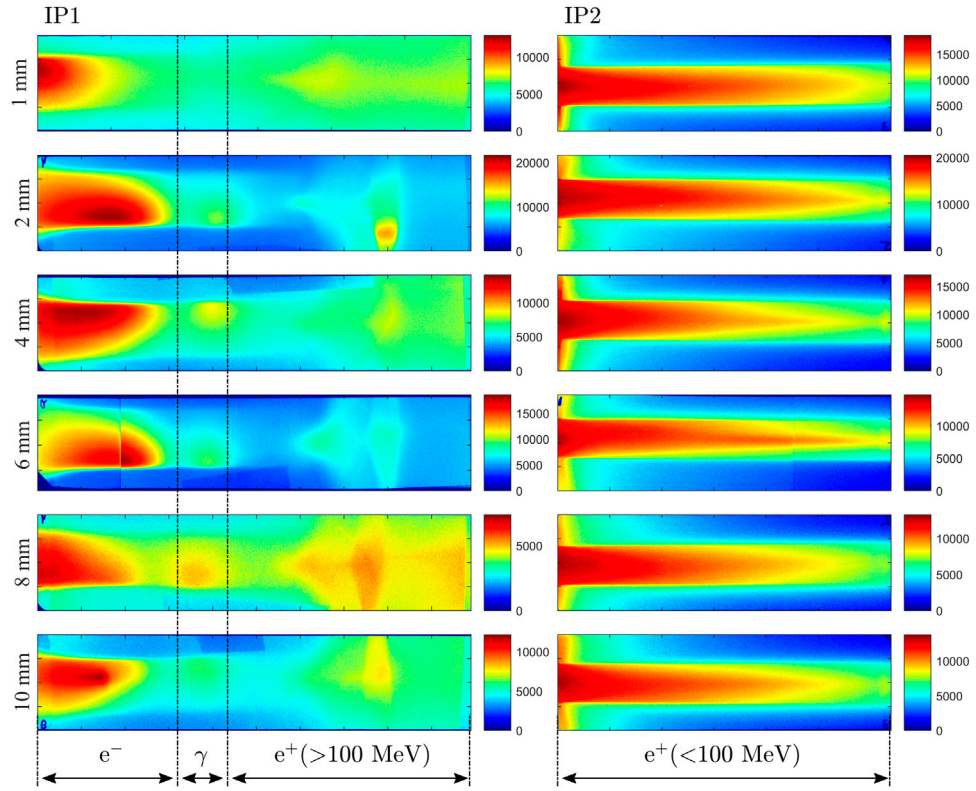

FIGURE 6
Raw information on particles recorded onto IP1 (in front of the magnetic spectrometer) and IP2 (on the side of the magnetic spectrometer) with a monolayer target of different thicknesses.

collimator was used to separate and spectrally resolve electrons, photons, and positrons from each other; then, these secondary particles could be recorded onto Image Plate 1 (IP1) located 10 cm after the magnetic spectrometer. Meanwhile, another Image Plate 2 (IP2) was tightly attached to the side of the magnetic spectrometer to record the low-energy positrons with a smaller deflection radius. The recorded information on all secondary particles with five shots at a monolayer target of different thicknesses is shown in Figure 6.

The outgoing positrons were mainly concentrated in the low-energy region (<100 MeV), while the energetic positrons (>100 MeV) accounted for only a small fraction (about 10%). The simulation results normalized to the actual experimental results are shown in Figure 7. It has a good agreement in the recorded positrons (marked with a black line and red line). The positrons recorded onto IP2 are about 1.47×10^7/shot for an 8-mm monolayer target, while the outgoing positrons are about 1.26×10^8/shot.

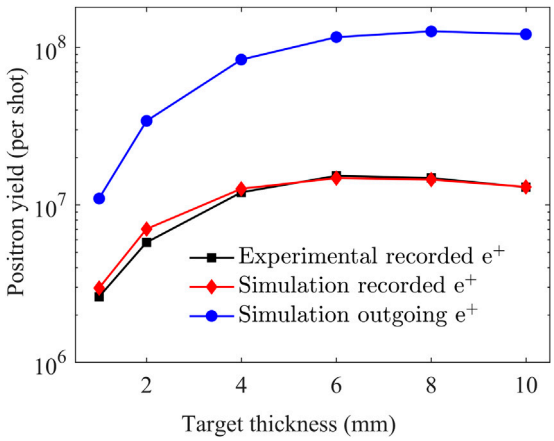

FIGURE 7
Comparison of experimental and simulation positrons with a monolayer target of different thicknesses.

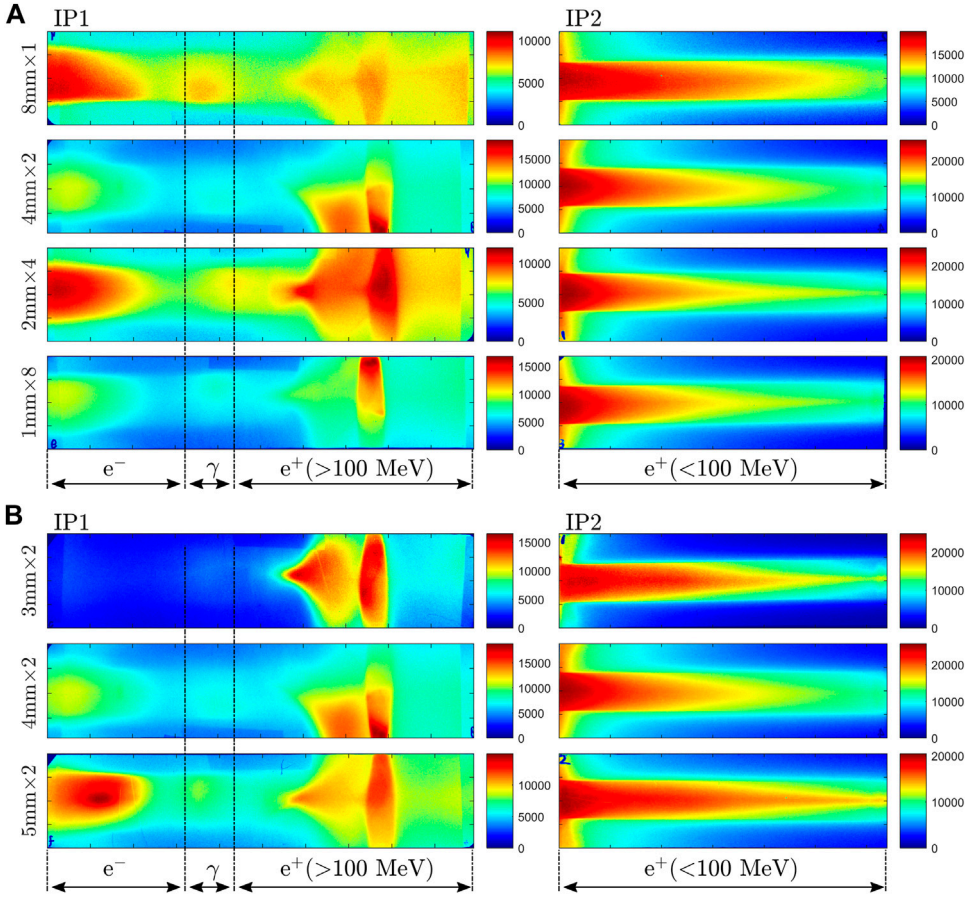

FIGURE 8
Raw information on particle signals obtained by IP1 (in front of the magnetic spectrometer) and IP2 (side of the magnetic spectrometer) with multi-layer targets. **(A)** Total thickness of multi-layer targets of 8 mm. **(B)** Bilayer targets.

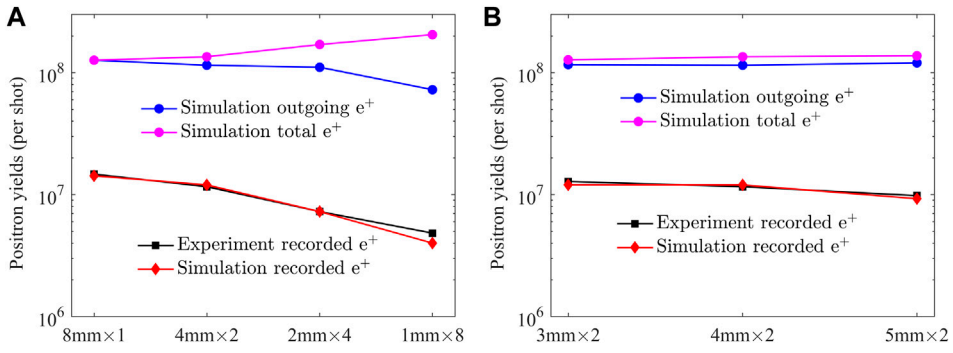

FIGURE 9
Comparison of experimental and simulation positrons with multi-layer targets. **(A)** Total thickness of multi-layer targets of 8 mm. **(B)** Bilayer targets.

Multi-layer target scheme

Based on the aforementioned discussion, we have experimentally studied the positron enhancement with multi-layer targets. The sketch of the experimental setup was, thus, essentially identical to the aforementioned target, with the only difference that we used multi-layer targets instead of a monolayer target. The raw information on particles obtained by IP1 and IP2 with five shots is shown in Figure 8, and the normalized simulation results based on the actual experimental setup are shown in Figure 9. The proportion of escaped positrons in the total positrons, which was the difference between the total positrons and outgoing positrons, as shown in Figure 9A, increased with the target thickness when the total thickness of multi-layer targets was 8 mm. The maximum yield of the total positrons obtained with eight-layer 1-mm targets (1 mm × 8) is about 2.1 × 10^8/shot, 62% higher than that of the outgoing positrons produced by an 8-mm monolayer target. The total positrons and outgoing positrons have the same trend with an increase in the target thickness in the scheme of bilayer targets (see Figure 9B). The total positrons and outgoing positrons increased with target thickness, while the scenario was reversed for the recorded positrons. The total positrons (1.38 × 10^8/shot) under bilayer 5-mm targets have increased by 14% compared to the outgoing positrons produced by an 8-mm monolayer target. To further optimize the positron yields under multi-layer targets, the thickness of the subsequent target and distance should be adjusted according to the intensity and angular distribution of positrons emitted from the previous target.

Conclusion

In summary, we have made an extensive study on the multi-layer targets and monolayer targets for positron enhancement. Using the energetic electron beam generated by the interaction of an ultra-intense laser and gas target as a discussion situation, we studied the transportation of electrons and electron-induced secondary particles in a tungsten target with the Geant4 code. By optimizing the multi-layer target structure, positrons with larger scattering angles can escape from the target zone, decreasing the annihilation of the electron–positron pair, thereby increasing the total positrons. The total positrons and FWHM of the outgoing positron beam increase with the target number using the thin target. However, adding the high-Z converter will prevent more positrons from entering the magnetic field, reducing the recorded positrons. Combining the experimental and simulation results, the total positrons under bilayer 5-mm targets (5 mm × 2) are up to 1.38 × 10^8/shot, 14% higher than the outgoing positrons (1.26 × 10^8/shot) under an 8-mm monolayer target. The size, thickness, number, and distance of every target should be deeply optimized according to the intensity and angular distribution of positrons emitted from the previous target.

Data availability statement

The data that support the findings of this study are available from the corresponding authors upon request.

Author contributions

MP conducted the simulations and drafted the manuscript. MP, B-YL, and Y-YM conducted the whole experiment. Y-YM supervised the work. All authors discussed the results and reviewed the manuscript.

Funding

This work was supported by the National Natural Science Foundation of China (Grant No. 11975308), the Open Fund of the State Key Laboratory of High Field Laser Physics (Shanghai Institute of Optics and Fine Mechanics), the Strategic Priority Research Program of Chinese Academy of Science (Grant No. XDA25050200), and the fund of Science Challenge Project (No. TZ2018001).

Acknowledgments

X-HY also acknowledges the financial support from the Fund for NUDT Young Innovator Awards (No. 20180104). JJ acknowledges the financial support from Fund for Hunan Provincial Natural Science Foundation of China (No. 2021JJ40654).

Conflict of interest

The authors declare that the research was conducted in the absence of any commercial or financial relationships that could be construed as a potential conflict of interest.

Publisher's note

References

1. Nakamura T, Hayakawa T. Quasi-monoenergetic positron beam generation from ultra-intense laser-matter interactions. *Phys Plasmas* (2016) 23(10):103109. doi:10.1063/1.4965914

2. Miyamoto K. *Plasma physics and controlled nuclear fusion*. Berlin, Heidelberg: Springer (2005).

3. Phelps ME, Cherry SR, Dahlbom M. *Pet: Physics, instrumentation, and scanners*. New York: Springer (2006).

4. Geise G. Positron annihilation spectroscopy. In: *Encyclopedia of membranes*. Berlin, Germany: Springer (2016).

5. Shearer JW, Garrison J, Wong J, Swain JE. Pair production by relativistic electrons from an intense laser focus. *Phys Rev A (Coll Park)* (1973) 1(-1):1582–8. doi:10.1103/physreva.8.1582

6. Strickland D, Mourou G. Compression of amplified chirped optical pulses. *Opt Commun* (1985) 56(3):447–9. doi:10.1016/0030-4018(85)90151-8

7. Liang EP, Wilks SC, Tabak M. Pair production by ultraintense lasers. *Phys Rev Lett* (1998) 81(22):4887–90. doi:10.1103/physrevlett.81.4887

8. Gryaznykh DA, Kandiev YZ, Lykov VA. Estimates of electron-positron pair production in the interaction of high-power laser radiation with high-Z targets. *Jetp Lett* (1998) 67(4):257–62. doi:10.1134/1.567660

9. Nakashima K, Takabe H. Numerical study of pair creation by ultraintense lasers. *Phys Plasmas* (2002) 9(5):1505–12. doi:10.1063/1.1464145

10. Shkolnikov PL, Kaplan AE, Pukhov A, Meyer-ter-Vehn J. Positron and gamma-photon production and nuclear reactions in cascade processes initiated by a sub-terawatt femtosecond laser. *Appl Phys Lett* (1997) 71(24):3471–3. doi:10.1063/1.120362

11. Shen B, Meyer-ter-Vehn J. Pair andγ-photon production from a thin foil confined by two laser pulses. *Phys Rev E* (2001) 65(1):016405. doi:10.1103/physreve.65.016405

12. Berezhiani VI, Garuchava DP, Shukla PK. Production of electron–positron pairs by intense laser pulses in an overdense plasma. *Phys Lett A* (2007) 360(4):624–8. doi:10.1016/j.physleta.2006.08.048

13. Myatt J, Delettrez JA, Maximov AV, Meyerhofer DD, Short RW, Stoeckl C, et al. Optimizing electron-positron pair production on kilojoule-class high-intensity lasers for the purpose of pair-plasma creation. *Phys Rev E* (2009) 79(6):066409. doi:10.1103/physreve.79.066409

14. Gahn C, Tsakiris GD, Pretzler G, Witte KJ, Delfin C, Wahlstrom CG, et al. Generating positrons with femtosecond-laser pulses. *Appl Phys Lett* (2000) 77:2662–4. doi:10.1063/1.1319526

15. Sarri G, Poder K, Cole JM, Schumaker W, Di Piazza A, Reville B, et al. Generation of neutral and high-density electron-positron pair plasmas in the laboratory. *Nat Commun* (2015) 6:6747. doi:10.1038/ncomms7747

16. Sarri G, Schumaker W, Di Piazza A, Vargas M, Dromey B, Dieckmann ME, et al. Table-Top laser-based source of femtosecond, collimated, ultrarelativistic positron beams. *Phys Rev Lett* (2013) 110(25):255002. doi:10.1103/physrevlett.110.255002

17. Sarri G, Schumaker W, Di Piazza A, Poder K, Cole JM, Vargas M, et al. Laser-driven generation of collimated ultra-relativistic positron beams. *Plasma Phys Control Fusion* (2013) 55:124017. doi:10.1088/0741-3335/55/12/124017

18. Chen H, Fiksel G, Barnak D, Chang PY, Heeter RF, Link A, et al. Magnetic collimation of relativistic positrons and electrons from high intensity laser–matter interactions. *Phys Plasmas* (2014) 21(4):040703. doi:10.1063/1.4873711

19. Chen H, Wilks SC, Bonlie JD, Chen SN, Cone KV, Elberson LN, et al. Making relativistic positrons using ultraintense short pulse lasers. *Phys Plasmas* (2009) 16:122702. doi:10.1063/1.3271355

20. Chen H, Wilks SC, Bonlie JD, Liang EP, Myatt J, Price DF, et al. Relativistic positron creation using ultraintense short pulse lasers. *Phys Rev Lett* (2009) 102:105001. doi:10.1103/physrevlett.102.105001

21. Cowan TE, Perry M, Key M, Ditmire T, Hatchett S, Henry E, et al. High energy electrons, nuclear phenomena and heating in petawatt laser-solid experiments. *Laser Part Beams* (1999) 17(4):773–83. doi:10.1017/s0263034699174238

22. Chen H, Wilks SC, Meyerhofer DD, Bonlie J, Chen CD, Chen SN, et al. Relativistic quasimonoenergetic positron jets from intense laser-solid interactions. *Phys Rev Lett* (2010) 105(1):015003. doi:10.1103/physrevlett.105.015003

23. Chen H, Nakai M, Sentoku Y, Arikawa Y, Azechi H, Fujioka S, et al. New insights into the laser produced electron–positron pairs. *New J Phys* (2013) 15(6):065010. doi:10.1088/1367-2630/15/6/065010

24. Gahn C, Tsakiris GD, Pretzler G, Witte KJ, Thirolf P, Habs D, et al. Generation of MeV electrons and positrons with femtosecond pulses from a table-top laser system. *Phys Plasmas* (2002) 9(3):987–99. doi:10.1063/1.1446879

25. Agostinelli S, Allison J, Amako K, Apostolakis J, Araujo H, Arce Dubois P, et al. Geant4—A simulation toolkit. *Nucl Instr Methods Phys Res A* (2003) 506(3):250–303. doi:10.1016/S0168-9002(03)01368-8

26. Allison J, Amako K, Apostolakis J, Araujo H, Arce Dubois P, Asai M, et al. Geant4 developments and applications. *IEEE Trans Nucl Sci* (2006) 53(1):270–8. doi:10.1109/TNS.2006.869826

27. Lei F, Jing J, Yan-Yun M, Zi-Jia Z, Yi-Fei L, Jun-Hao T, et al. High stability positron beam generation based on ultra-intense laser. *Acta Phys Pol A* (2020) 137(2):156–9. doi:10.12693/aphyspola.137.156